Ecosystems (2019) 22: 1308–1324
https://doi.org/10.1007/s10021-019-00337-1

Nitrogen Retention of Terricolous Lichens in a Northern Alberta Jack Pine Forest

Adam Bird,[1]* Shaun A. Watmough,[2] Michael A. Carson,[3] Nathan Basiliko,[3] and Andrew McDonough[1]

[1]*Environmental and Life Sciences Graduate Program, Trent University, Peterborough, Ontario K9L 0G2, Canada;* [2]*Trent School of The Environment, Trent University, Peterborough, Ontario K9L 0G2, Canada;* [3]*Department of Biology, Vale Living with Lakes Centre, Laurentian University, Sudbury, Ontario P3E 2C6, Canada*

Abstract

The Athabasca Oil Sands in Alberta, Canada, is one of the largest point sources of nitrogen oxides in Canada. There are concerns that elevated nitrogen (N) deposition will adversely impact forest ecosystems located downwind of emission sources. The role of the forest floor in regulating these potential eutrophication effects was investigated following a 5-year enrichment study in which N was applied as NH_4NO_3 above the canopy of a jack pine (*Pinus banksiana* Lamb) stand in northern Alberta close to Fort McMurray at rates ranging from 5 to 25 kg N ha^{-1} y^{-1} in addition to background deposition of approximately 2 kg N ha^{-1} y^{-1}. Chemical analysis of lichen mats revealed that the N concentration in the apical (upper) lichen tissue and necrotic tissue increased with treatment. When expressed as a N pool, the fibric–humic material held the largest quantity of N across all treatments due to its relatively large mass (172–214 kg N ha^{-1}), but there was no significant treatment effect. Soil net N mineralization and net nitrification rates did not differ among N treatments after five years of application. A ^{15}N tracer applied to the forest floor showed that N is initially absorbed by the apical lichen (16.6% recovery), FH material (29.4% recovery), and the foliage of the vascular plant *Vaccinium myrtilloides* (31.7% recovery) in particular. After 2 years, the FH ^{15}N pool size was elevated and all other measured pools were depleted, indicating a slow transfer of N to the FH material. Applied ^{15}N was not detectable in mineral soil. The microbial functional gene ammonia monooxygenase (*amoA*) responsible for catalyzing the first step in nitrification was undetectable using PCR screening of mineral soil microbial communities in all treatments, and broad fungal/bacterial qPCR assays revealed a weak treatment effect on fungal: bacterial ratios in mineral soil with decreasing relative fungal abundance under higher N deposition. This work suggests that terricolous lichen mats, which form the majority of ground cover in upland jack pine systems, have a large capacity to effectively retain elevated N deposition in soil humus.

Key words: nitrogen; oil sands; eutrophication; lichens; nitrogen saturation.

Received 14 August 2018; accepted 16 December 2018;
published online 31 January 2019

Author Contributions AB wrote the paper, performed field research, performed laboratory analysis, and analyzed data; SAW conceived of study and edited paper; NB contributed laboratory facilities, designed microbial methodology, and edited paper; MAC designed microbial methodology, performed laboratory analysis, and edited paper; AM designed isotope experiment, performed field research, and edited paper.

**Corresponding author; e-mail:* adambird@trentu.ca

Introduction

Anthropogenic activity in the last 100 years has had dramatic effects on the planet's nitrogen (N) cycle (Galloway and others 2004). Terrestrial ecosystems that developed in N-limiting environments have adapted to N scarcity. In these systems, the sudden addition of surplus N has been shown to cause changes in vegetation community composition, loss of sensitive species, lower soil C:N ratios leading to increases in soil N mineralization and nitrification rates, and increases in soil nitrate (NO_3^-) leaching (Aber and others 1989). In the 1980s, elevated atmospheric N deposition was identified as a potential stressor on the health of forests in Europe (Nihlgard 1985) and eastern North America (Aber and others 1989). The theory of N saturation seeks to explain the expected responses of an ecosystem as excess N is added. Nitrogen saturation is defined as: ''The state reached when bioavailable forms of N are present in excess of current biological demand'' (Aber and others 1989). This formalized theory of N saturation was derived primarily from experiments in the northeastern forests of the USA and is conceptualized as a linear progression through four distinct phases as a system experiences chronic atmospheric N loading. Under Aber's model, N saturation can be readily determined by biogeochemical changes in soil processes that include increased N availability and leaching of NO_3^- below the rooting zone (Aber and others 1989). Increased NO_3^- leaching may lead to soil acidification, and N accumulation in soils may ultimately result in changes in plant species (Aber and others 1989; Driscoll and others 2003).

Working under Aber's model, many studies have been performed on ecosystems in North America and Europe to try to explain the process of N saturation (Tietema and others 1998a; Fenn and others 2003). Gradient studies that take advantage of existing spatial differences in atmospheric N deposition have been widely used to measure responses in soil processes and changes in plant community composition (Mitchell and others 2005; Akselsson and others 2010). Nitrogen enrichment experiments using forest floor and canopy applications of various N forms have been performed to establish dose–response relationships (Wright and van Breemen 1995). In addition, ^{15}N natural abundance studies have been performed, which use the natural microbial fractionation of N isotopes to detect responses to N saturation (Emmett and others 1998; Pardo and others 2006), and ^{15}N isotope tracer studies have been performed to determine the fate and fluxes of elevated N inputs (Robinson 2001; Templer and others 2012). Studies have also been conducted investigating the role of soil microbial communities in N cycling directly, for example, through microbial biomass assays targeting broad groups (for example, fungi and bacteria), and the characterization of functional genes of specific microbial guilds instrumental in N cycling (Demoling and others 2008; Levy-Booth and others 2014). Measurements of fungal and bacterial biomass under chronic N addition in the northeastern USA have shown that microbial biomass can decrease by as much as 50% under deposition rates of about 30 kg ha^{-1} y^{-1} for 10 years (Wallenstein and others 2006).

In 2011, Lovett and Goodale proposed a revised conceptual model of N saturation. The main distinction between the two models is that Lovett and Goodale (2011) made a distinction between capacity N saturation and kinetic N saturation. Capacity N saturation occurs when a pool has accumulated as much N as possible, and additional N is no longer retained. Kinetic N saturation occurs when the rate of N input is greater than the maximum accumulation rate of a pool. When a pool is undergoing kinetic N saturation, it is possible to have both N accumulation and N loss from a pool simultaneously. The Lovett–Goodale model therefore explains some of the incongruities seen in N saturation studies (for example, increases in NO_3^- leaching without increases in foliar N concentration), by allowing N to accumulate in pools, and exit pools simultaneously, according to the diverse circumstances of the systems in question.

The Athabasca Oil Sands Region (AOSR) in northern Alberta, Canada, is located in the boreal plains ecozone and is experiencing rapid industrial growth. The operation of large fleets of diesel-powered heavy equipment and upgrader facilities both produce large quantities of NO_x emissions in the region (Bytnerowicz and others 2010). In the AOSR, NO_x emissions increased from 148 t d^{-1} to 310 t d^{-1} between 2003 and 2011 (Fenn and others 2015). Total N deposition near the highly industrialized areas of the AOSR has been measured at rates in excess of 25 kg ha^{-1} y^{-1} (Fenn and others 2015). There are concerns that NO_x emissions and subsequent NH_4–N and NO_3–N deposition will continue to rise as oil sands development expands, potentially having adverse effects to adjacent ecosystems associated with N saturation. Jack pine (*Pinus banksiana* Lamb.) forests typically grow in coarse-textured, upland soils. The combination of low background deposition, nutrient-poor soils, and sensitive biological communities makes these

forests particularly sensitive to the effects of increased N deposition (Högberg and others 2003; Allison and others 2008).

A distinctive feature of the ground-cover community in these systems is the dominance of terricolous lichen species, mainly ''reindeer lichens'' *Cladonia mitis* and *Cladonia stellaris*. Lichens do not possess rooting structures and are therefore incapable of accessing soil nutrient pools; instead, their nutrient requirements are met largely through atmospheric deposition (Ellis and others 2003). Mat-forming lichens have a particularly advantageous ability to translocate nutrients from necrotic tissue to their apical tissue, therefore increasing nutrient use efficiency and growth rates in nutrient-scarce environments (Crittenden 1991; Hyvärinen and Crittenden 1998). Due to their specialized adaptions to low N environments, lichens also find themselves susceptible to the effects of surplus N deposition and eutrophication. For terricolous lichens such as *Cladonia mitis* and *Cladonia stellaris*, the threat is twofold: direct toxicity of excess N and competition from vascular plants that are more tolerant of high N environments (Cornelissen and others 2001; Munzi and others 2017).

Given the expected sensitivity of upland soils and terricolous lichen communities, we initiated an experimental N application study in 2011 to assess the impacts of elevated N deposition and subsequent N saturation processes on upland Jack pine forests. Six experimental plots were established, and N was applied aerially over the canopy via helicopter as ammonium nitrate (NH_4NO_3) at treatment levels consistent with current and future predicted N deposition levels in the region. In this study, we stratified lichen mats by depth and compared the N concentration and pool size between experimental N treatments after 5 years of N application. We also conducted an ^{15}N tracer study on ground plots to identify N mobility pathways within the forest floor, compared fungal and bacterial abundance among treatments, and screened for the microbial functional gene ammonia monooxygenase (*amoA*) which is involved in the first step of nitrification.

Materials and Methods

This study was conducted at a 65-year-old upland jack pine forest located 46 km north of the city of Fort McMurray in northern Alberta, Canada (57°7′16.66″N, 111°25′41.39″W) (Fig. 1). The

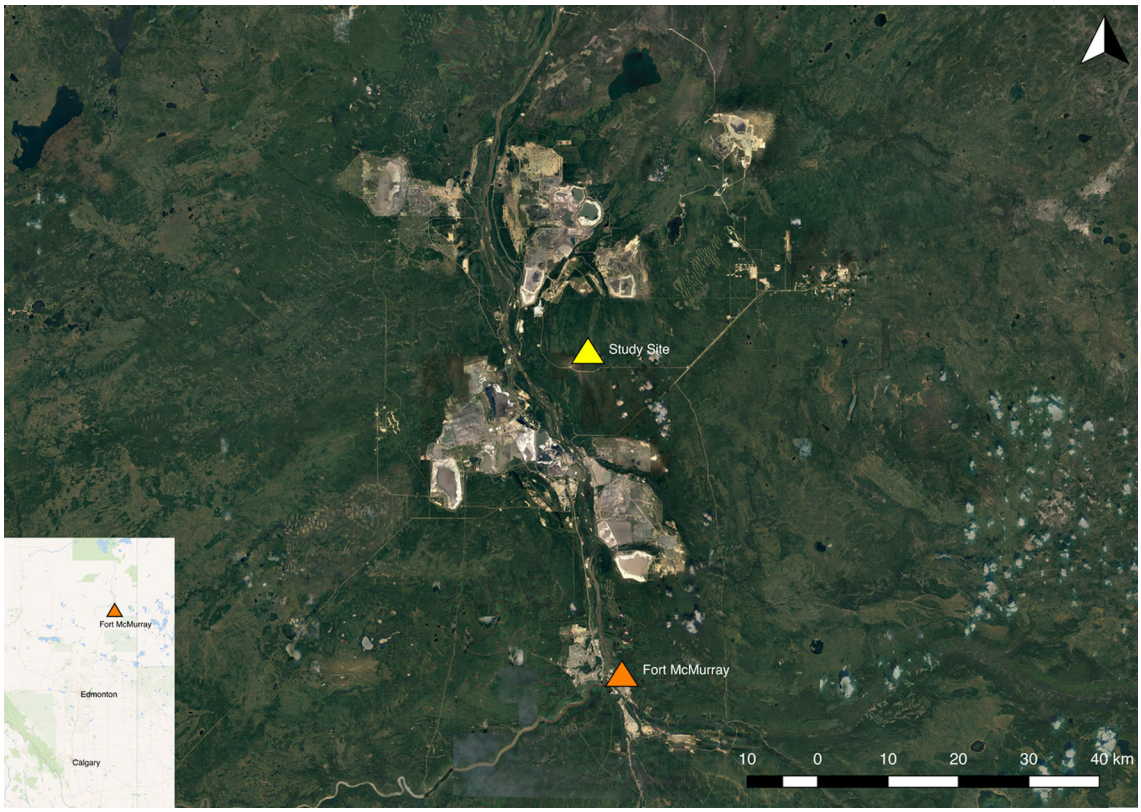

Fig. 1. Regional map of AOSR and location of study site.

average annual precipitation from 2011 to 2015 was 456 mm y^{-1} (Environment Canada, 2015). The average minimum temperature during the growing season from 2011 to 2015 (May–September) was 7.4 °C, and the average maximum temperature was 21.2 °C (Environment Canada 2011). The forest floor community is dominated by mat-forming lichen species (*Cladonia mitis, Cladonia. stellaris)* and dwarf shrubs (*Vaccinium vitis-idaea, Vaccinium myrtilloides, Arctostaphylos uva-ursi)*. The soils are coarse sandy Brunisols (Soil Classification Working Group 1998). Background atmospheric inorganic N deposition in the area is approximately 2 kg ha^{-1} y^{-1} (Watmough and others 2014). Soils at the study site were nearly pure sand, with very low clay and soil organic matter (SOM) content; the SOM concentration of the Ae and B horizons was between 0.74–5.74% in the Ae horizon, and 0.05–2.6% in the B horizon. The cation exchange capacity (CEC) is low and was much higher in the LFH than in the Ae horizon of the mineral soil, ranging from 38.27 to 78.12 meq 100 g^{-1}, whereas the CEC in the Ae horizon ranged from 8.81 to 18.69 meq 100 g^{-1}. Base saturation (BS) was higher also in the LFH than in the Ae horizon, although the difference was not as large as the difference in CEC, ranging from 11.45 to 23.44% in the LFH, and from 8.55 to 16.75% in the Ae horizon (Table 1).

Nitrogen Enrichment Procedures

Nitrogen applications were performed over the forest canopy four times during the growing period (May, June, July, and September) between the years 2011–2015. Aerial applications were chosen to properly integrate the effects of canopy interactions on N cycling. Monitoring studies in the region have shown that atmospheric deposition of NO_3–N and NH_4–N is similar, and N deposition can be as high as 25 kg N ha^{-1} y^{-1} (Fenn and others 2014; Watmough and others 2014) Nitrogen was therefore applied as aqueous NH_4NO_3 at deposition rates consistent with current and projected future atmospheric deposition in the region (0, 5, 10, 15, 20, and 25 kg N ha^{-1} y^{-1}) in addition to ambient N deposition of 2 kg N ha^{-1} y^{-1}. These deposition loads also encompass the range of current European critical loads for boreal ecosystems (Bobbink and others 2010). Six plots were established in the site with the dimensions 80 m × 20 m. Each plot received 100L of solution per application, which is equivalent to an increase in precipitation of 0.06 mm (or < 1% of annual precipitation). In June 2014, 60, 25 × 25 cm plots were randomly

Table 1. Background Soil Characteristics at Treatment Sites in 2015

		Treatment (kg N ha^{-1} y^{-1})						P =
		0 (2)	5 (7)	10 (12)	15 (17)	20 (22)	25 (27)	
Base saturation (%)	LFH	11.45 ± 2.11	17.99 ± 1.49	22.33 ± 3.27	20.66 ± 5.86	23.44 ± 4.46	15.09 ± 1.59	N.S
	Ae	8.55 ± 1.50	16.75 ± 5.26	11.14 ± 2.15	12.55 ± 2.60	15.17 ± 4.65	9.28 ± 2.67	N.S
pH	LFH	4.75 ± 0.07	4.72 ± 0.08	4.94 ± 0.08	5.02 ± 0.11	4.87 ± 0.08	4.95 ± 0.12	N.S
	Ae	4.87 ± 0.10	4.76 ± 0.14	5.05 ± 0.10	4.93 ± 0.08	4.85 ± 0.09	4.96 ± 0.12	N.S
	B	5.42 ± 0.07	5.43 ± 0.14	5.48 ± 0.14	5.41 ± 0.10	5.28 ± 0.03	5.23 ± 0.08	N.S
C/N ratios	LFH	41.77 ± 2.31	43.64 ± 3.61	34.45 ± 0.73	37.27 ± 1.00	39.90 ± 3.53	32.73 ± 1.26	N.S
	Ae[1]	41.48 ± 4.99	42.36 ± 4.07	44.78 ± 3.19	35.25 ± 5.76	29.16 ± 1.62	38.01 ± 3.19	N.S
	B[2]	24.76 ± 4.83	22.28 ± 3.38	30.46 ± 4.44	14.17 ± 1.39	14.29 ± 0.88	29.85 ± 3.90	< 0.05

Values in brackets represent total deposition to the area (background + experimental addition). ± represents standard error.
[1]C/N ratios for Ae horizon were derived from [N] values below instrument quantification limit.
[2]C/N ratios for B horizon were derived from [N] values and [C] values below instrument quantification limit.

established on the forest floor for a separate ^{15}N experiment (sites had received no N treatment). Half of the plots (n = 30) were treated a single time with ^{15}N isotope in the form of aqueous double-labeled ammonium nitrate ($^{15}NH_4^{15}NO_3$) equivalent to a deposition load of 25 kg N ha^{-1} y^{-1} (98 atom % ^{15}N). Tracer applications were performed using a handheld spray bottle at a height of about 25 cm above the forest floor.

Field Sample Collection

Dwarf shrub biomass was collected from the treated plots during June 2015 (during the 5th year of N application), including *Arctostaphylos uva-ursi, Vaccinium myrtilloides,* and *Vaccinium vitis-idaea*. Dwarf shrub foliage was removed from the stem and collected. All dwarf shrub biomass was transported in paper bags and returned to the laboratory for further processing. One sample of each biomass type was collected per treatment subplot (3 per plot, 18 total).

During the final year (2015) of N applications, net N mineralization and nitrification rates were measured in soil underneath terricolous lichen mats using the buried bag method (Hart and others 1994). Two soil cores measuring 10 cm deep were extracted adjacent to one another and placed into sealed polyethylene bags. One bag was returned to the laboratory for chemical analysis to determine the initial concentrations of NH_4 and NO_3^-. The second bag was left in situ and analyzed after approximately 1 month. This process was repeated 4 times during the growing season (May–June, June–July, July–September, and September–October). Sample bags were kept refrigerated at or below 5 °C prior to processing and analysis. In the final year of N application (2015) as well as one year after applications ceased (2016), complete lichen mats (all lichen and organic material above the mineral soil) were collected using plastic containers of known area and volume from each treatment plot. Six replicates were sampled from each treatment plot (n = 36) at four times throughout the study period: May 2015, July 2015, September 2015, and in August 2016 one year after N application ceased (n = 144).

In the final year of N application (2015), mineral soil was collected from each treatment subplot for soil microbial analysis. Lichen mats were removed from the forest floor, and debris was cleared using a trowel. Between 5 and 10 g of mineral soil was collected from the first 2 cm of the soil. Five random samples were taken from each treatment destructive subplot (n = 15 per treatment plot, n = 90 total). Soil collection occurred in May, July, and September of 2015. Soil samples were kept frozen at -20 °C until analysis.

Ten ^{15}N-treated plots and 10 untreated plots were destructively sampled 24 hours following application to determine the initial distribution of the applied N throughout biomass, and soil pools. *C. mitis* lichen mats were collected using the same method described above. The foliage of the dwarf shrubs *Arctostaphylos uva-ursi*, *Vaccinium vitis-idaea*, and *Vaccinium myrtilloides* was sampled. Mineral soil from the Ae and B horizons was also collected from the area directly below the site of complete lichen mat removal. This destructive sampling was repeated in summer 2015 and summer 2016 on the remaining ground plots.

Laboratory Analysis

Biomass Samples

Biomass samples were oven-dried at 60 °C for 72 hours. Complete lichen mat samples from both the aerial applications and the ^{15}N tracer sites were carefully separated into apical lichen (top 2 cm), necrotic lichen (lower section of lichen thallus), and fibric–humic (FH) material. All lichen mat mass was retained and recorded. Dried and sorted samples were pulverized in a fine powder using an analytical mill. Biomass samples from the aerial application experiment were analyzed for C, N, and sulfur (S), using an Elementar Vario Macro dry combustion analyzer. National Institute of Standards and Technology (NIST) 1515 apple leaf standards were prepared and combusted at a rate of 1 for every 20 samples to ensure adequate analyte recovery. ^{15}N-treated replicates and 3 untreated replicates were randomly selected from each collection year and each N pool for analysis. ^{15}N-treated biomass and soil samples from all plots were analyzed using a continuous-flow isotope ratio mass spectrometer. Typical precision of replicate analyses was usually within 0.3‰

Soil Samples

Refrigerated mineralization/nitrification soil samples were removed from the bags and passed through a 2-mm sieve to remove any non-soil debris. Two approximately 4 g subsamples were taken: one for NH_4^+ analysis and one for NO_3^-. NH_4^+ extraction was performed using 2 M KCl, and NO_3^- extraction was performed using deionized water (Dick and Tabatabai 1979). Extracted NH_4^+ and NO_3^- samples were analyzed using an auto-analyzer and ion chromatography, respectively.

Frozen soil samples were subsampled (1 g from each) and homogenized into a 5-g composite subplot sample (n = 18 per time interval) for microbial analyses. DNA was isolated in 0.5 g replicates of frozen soil using the Power Soil® Isolation Kit following the manufacturer's protocol (MoBio Laboratories Inc., Carlsbad, CA, USA Catalog #12888-100 Lot # PS 14H5). DNA concentration and purity were measured with a Synergy H1 microplate reader (BioTek Instruments Inc., Winooski, VT, USA Mfr. No. BioTek™ BTH1MD Catalog Number 11-120-534). Extracted DNA was homogenized and stored frozen until analysis.

A preliminary analysis for the *amoA* functional gene was performed using four DNA samples per season (12 total) from the two lowest and two highest treatment plots (0, 5, 20, 25 kg N ha^{-1} y^{-1}) and homogenized by subsampling 10 µl of each into a common tube. DNA extracted from forest soils along a roadside transect in southern Ontario was used *in lieu* of a positive control. DNA samples were diluted to 1/10 and 1/100 of original concentration. A series of PCRs were run using combinations of *amoA* forward and reverse primers (Rotthauwe and others 1997; Stephen and others 1999; Baptista and others 2014). Reactions were performed in 10 µl solutions containing 3.5 µl dH_2O, 5 µl Phire master mix, 0.5 µl of each primer, and 0.5µl DNA sample. The cycling protocol was 2 min at 98 °C followed by 40 cycles of 20 s at 98 °C, 20 s at 56–62 °C, 40 s at 72 °C and 4 min at 72 °C.

DNA samples were analyzed using qPCR with a Stratagene Mx300SP (Agilent Technologies Santa Clara, California) for absolute abundance of bacteria and fungi. For the bacteria, the primers bac331F (5′ TCC TAC GGG AGG CAG CAG T) and bac797R (5′ GGA CTA CCA GGG TCT AAT CCT GTT) were used (Nadkarni and others 2002). qPCRs were optimized using a preliminary PCR of a homogenized environmental sample with a thermal gradient and visual examination on a 1.5% agarose gel. A pure culture of *E. coli* (ATCC 11303) was used to create standards of known concentrations in a serial dilution. Four standards were prepared in triplicate at 1:10, 1:100, 1:1000, and 1:10000 dilution. qPCRs were performed in triplicate in 10 µl solutions containing 3 µl dH_2O, 5 µl SYBR® Green supermix with ROX (BioRad #172-5121), 0.5 µl of each primer, and 1 µl of DNA sample. The cycling protocol was 5 min at 95 °C followed by 40 cycles of 15 s at 95 °C, 30 s at 64 °C, 30 s at 72 °C. A dissociation curve was then generated in 1 °C increments from 64 to 95 °C. PCR products were confirmed via dissociation curves and verification on a 1.5% agarose gel. Similarly, for fungal abundance, DNA samples were analyzed using the primers ITS1F (5′ TCC GTA GGT GAA CCT GCG G) and 5.85R (5′ CGC TGC GTT CTT CAT CG) (Glass and Donaldson 1995; Fierer and Jackson 2005). A pure culture of *S. cerevisiae* (ATCC 2360) was used to create standards of known concentration in a serial dilution ranging from full concentration to 1:1000. Reactions were performed in triplicate, and reagent mixes and reaction conditions were identical to those in the bacterial run with the exception of primers and annealing/initial denaturation temperature which was raised to 61 °C.

Data Analysis

Statistical significance among treatments for parameters that were assessed multiple times throughout the season (mineralization rate, net nitrification rate, soil ammonium concentration, soil nitrate concentrations, apical/necrotic/FH lichen N concentration, apical/necrotic/FH lichen N pool, bacterial/fungal ratio) was tested using two-way repeated-measures ANOVA to account for the influence of broad seasonal drivers. Sorted lichen samples were also tested for statistical significance of all measured chemical parameters (N concentration, N pool size) within sampling periods (May 2015, July 2015, September 2015, and August 2016). Distributions were assessed via the Shapiro–Wilks normality test. Parametric distributions were analyzed using a one-way ANOVA and Tukey's HSD post hoc test. Nonparametric distributions were analyzed using a Kruskal–Wallis rank-sum test and Mann–Whitney post hoc test. ^{15}N tracer background and treatment samples were compared using t tests. Differences between ^{15}N enrichment years were assessed using one-way ANOVA and Tukey's HSD post hoc test. All analysis was performed in the R software environment using the base ''stats'' package (R Core Team 2017). All figures were produced in the R environment using the ''ggplot2'' package (Wickham 2016). Color palettes used in graphics were applied using the ''rColorBrewer'' package (Neuwirth 2014). Intermediate data manipulation was partially performed using the ''broom'' package (Robinson 2017).

Results

Net Nitrogen Mineralization and Nitrification

Soil net mineralization and net nitrification rates measured during the 2015 growing season (5th year of N additions) were highly variable over time

Table 2. Soil Net Mineralization Rate and Nitrification Rate During the 2015 Growing Season

		Treatment (kg N ha^{-1} y^{-1})						P =
		0 (2)	5 (7)	10 (12)	15 (17)	20 (22)	25 (27)	
Net mineralization rate (kg N ha^{-1} y^{-1})	May–June	0.98 ± 0.83	0.40 ± 0.36	0.12 ± 0.04	0.20 ± 0.08	0.20 ± 0 .05	0.20 ± 0.04	N.S
	June–July	28.20 ± 6.35	12.83 ± 13.72	− 32.20 ± 17.38	2.72 ± 32.13	0.54 ± 10.38	2.91 ± 60.91	
	July–Sept	25.92 ± 9.38	2.44 ± 9.45	− 16.55 ± 5.95	− 34.48 ± 15.69	− 11.10 ± 5.52	− 15.80 ± 4.48	
	September–October	− 3.14 ± 1.36	− 1.86 ± 1.00	− 9.89 ± 12.01	− 38.45 ± 11.97	− 4.01 ± 4.57	− 7.64 ± 16.45	
Net nitrification rate (kg N ha^{-1} y^{-1})	May–June	− 5.78 ± 1.27	− 9.97 ± 2.63	− 6.61 ± 2.56	− 5.87 ± 1.54	− 9.07 ± 7.52	− 5.95 ± 1.44	N.S
	June–July	0.50 ± 0.24	0.39 ± 0.11	− 0.19 ± 0.41	1.08 ± 10.00	3.22 ± 2.76	0.39 ± 0.57	
	July–September	0.10 ± 0.28	− 0.11 ± 0.29	0.64 ± 0.27	− 0.10 ± 0.25	0.32 ± 0.18	1.25 ± 1.07	
	September–October	0.98 ± 0.82	0.40 ± 0.36	0.18 ± 0.04	0.20 ± 0.8	0.20 ± 0.05	0.20 ± 0.04	

± *Represents standard error.*

and did not show a clear treatment effect (Table 2). Repeated-measures ANOVA showed that there was a seasonal effect on mineralization rate ($p < 0.05$) and a significant interaction between season and treatment ($p < 0.05$). The net mineralization rate measured from May to June was positive but extremely low and tended to increase with N treatment (0, 5, 15, 25 kg N ha^{-1} y^{-1}) from June to July. From July to September, net mineralization rates remained positive at the 0 and 5 kg ha^{-1} y^{-1} treatment rates, but were negative at 10 kg N ha^{-1} y^{-1} and above. From September to October, the net mineralization rate was negative in all treatments, with the lowest rate occurring at 15 kg N ha^{-1} y^{-1}. Repeated-measures ANOVA also showed that there was a seasonal effect on net nitrification rate ($p < 0.05$), but treatment did not have a statistically significant effect on nitrification rate. Growing season net mineralization rates were greater in magnitude than net nitrification rates, reaching maximum/minimum rates of ± 30 kg NH_4^+ N ha^{-1} y^{-1}, compared with net nitrification rates of − 10 kg NO_3^- N ha^{-1} y^{-1}. Net nitrification rates were negative from May to June at all treatment rates (Table 2). From June to July, net nitrification rates were positive at all treatment rates with the highest net nitrification rate occurring at 20 kg N ha^{-1} y^{-1}. Later in the year net nitrification rates were positive at all treatment rates but were all only marginally greater than zero.

Nitrogen Concentration and Pools in Terricolous Lichens after 5 Years of N Additions

Lichen N concentrations increased with N treatment in apical and necrotic lichen tissue, but the response was less strong in the FH material, which had the highest N concentration (Figure 2). Nitrogen concentrations in apical, necrotic and FH material also varied by season ($p < 0.05$ for all). Apical lichen N concentration ranged from a minimum of 0.52% in July 2015 in the control plot to a maximum of 1.09% in September 2015 in the highest N treatment. Similarly, necrotic lichen N concentration ranged from a minimum of 0.39% in September 2015 in the control plot to a maximum of 0.79% in September 2015 at the highest treatment. In contrast, the treatment effect evident in the FH material was more variable; the N concentration ranged from a minimum of 0.67% in August 2015 at the 5 kg N ha^{-1} y^{-1} treatment to a maximum of 1.10% in July 2015 at treatment rate 25 kg N ha^{-1} y^{-1}, but differences among treatment were only evident in July 2015 and August 2015 (Figure 2). Nitrogen con-

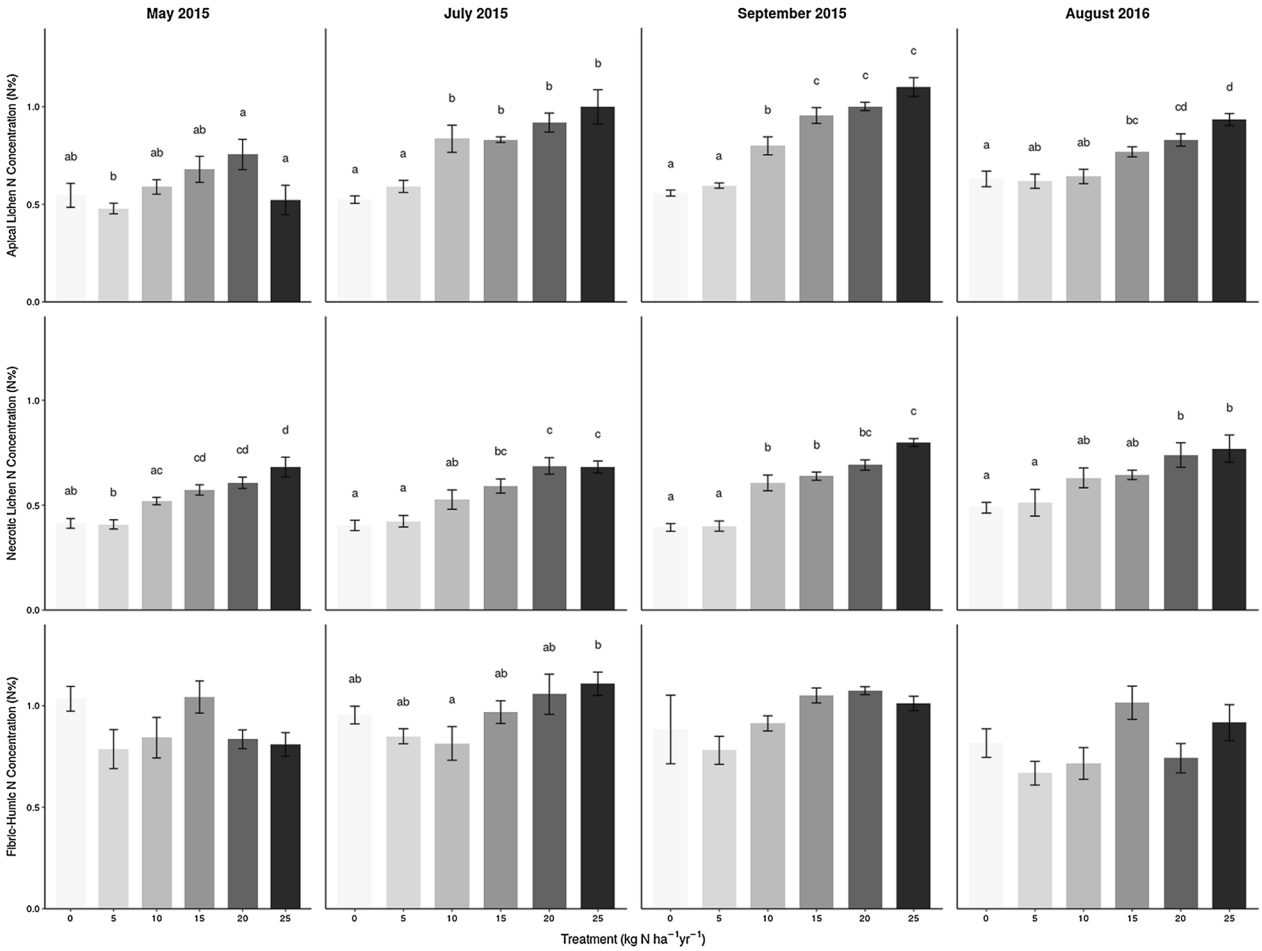

Fig. 2. N concentration of *Cladonia mitis* mats during the last year of N application (May 2015, July 2015, September 2015) and one year after applications ended (August 2016). Error bars represent standard error. Differing letters above columns represent statistical significance between groups.

centrations were slightly lower across high treatments (10 kg ha^{-1} y^{-1} and above) in all 3 lichen types in August 2016 compared with July and September 2015.

The N pool size associated with the ground lichen layer generally increased with treatment in the apical tissue and necrotic tissue ($p < 0.05$ for both), but there was no treatment effect in FH material (Figure 3). The N pool size in FH lichen was substantially larger than that of the apical and necrotic lichen due to the high mass of FH material. Even in the control plots, the FH pool was as much as 30 times greater than the apical tissue N pool and 10 times greater than the necrotic N pool depending on season. The apical lichen N pool size ranged from a minimum of 6.6 kg N ha^{-1} in May at treatment rate of 5 kg N ha^{-1} y^{-1} to a maximum of 13.7 kg N ha^{-1} in July at treatment rate 25 kg N ha^{-1} y^{-1}. The necrotic lichen N pool size ranged from a minimum of 9.4 kg N ha^{-1} in September in control plots to a maximum of 19.0 kg N ha^{-1} in September at the high N treatment. The N pool associated with the FH material was much larger and ranged from a minimum of 172 kg N ha^{-1} in August in the control plots to a maximum of 214 kg N ha^{-1} in September at treatment rate 15 kg N ha^{-1} y^{-1}. Apical lichen N pools were lower in 2016 at high treatment rates than in July and September of 2015.

Nitrogen Concentrations in Vascular Plants after 5 Years of N Additions

There were no statistically significant differences in foliar N concentration among treatments in the three dwarf shrub species: *V. vitis-idaea*, *V. myrtilloides*, and *A. uva-ursi* (Figure 4). However, all three dwarf shrubs had greater background foliar N concentrations than the lichens and bryophyte.

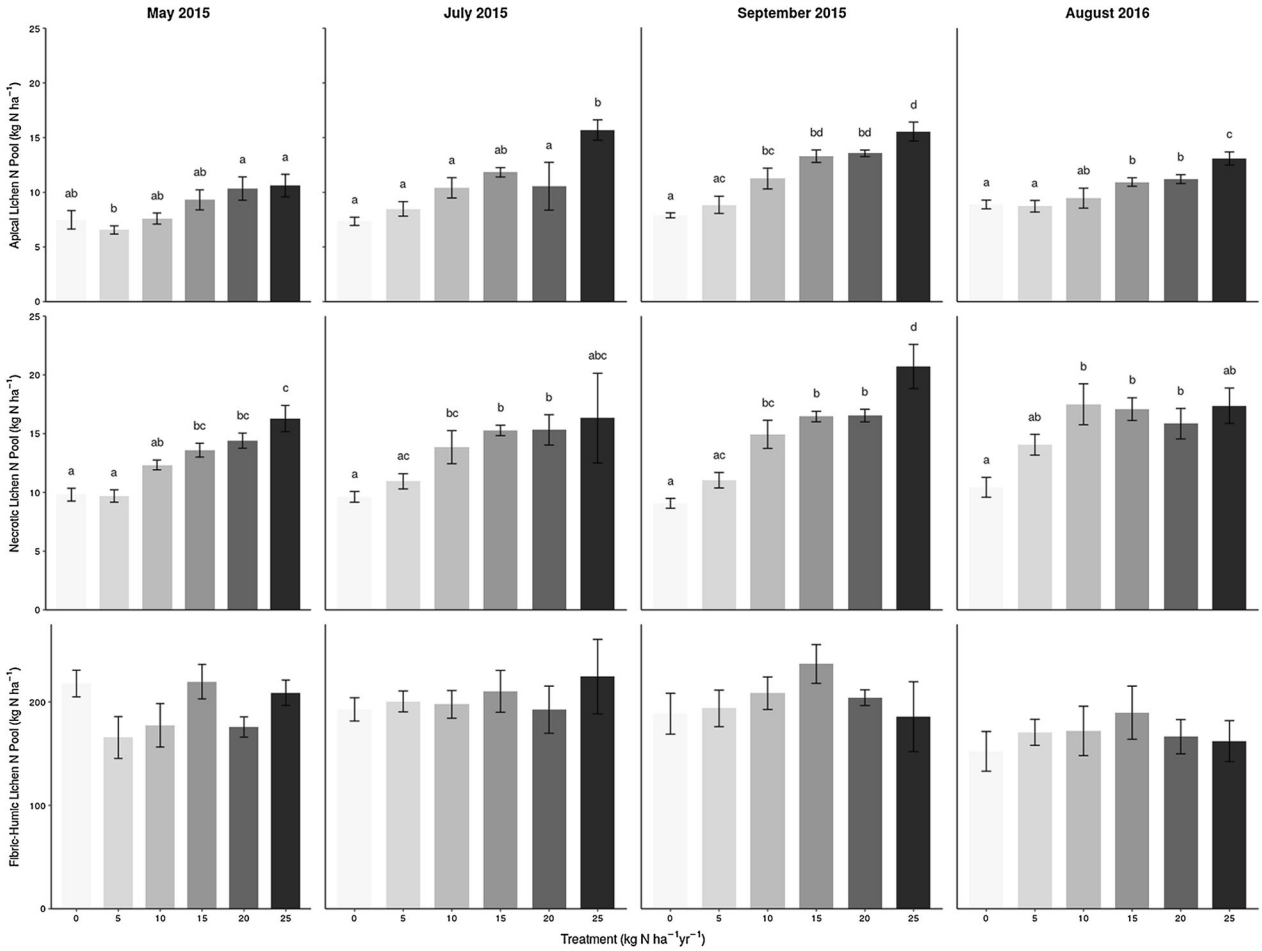

Fig. 3. Total N pools of *Cladonia mitis* mats during the last year of N application (May 2015, July 2015, September 2015) and one year after applications ended (August 2016). Error bars represent standard error. Differing letters above columns represent statistical significance between groups.

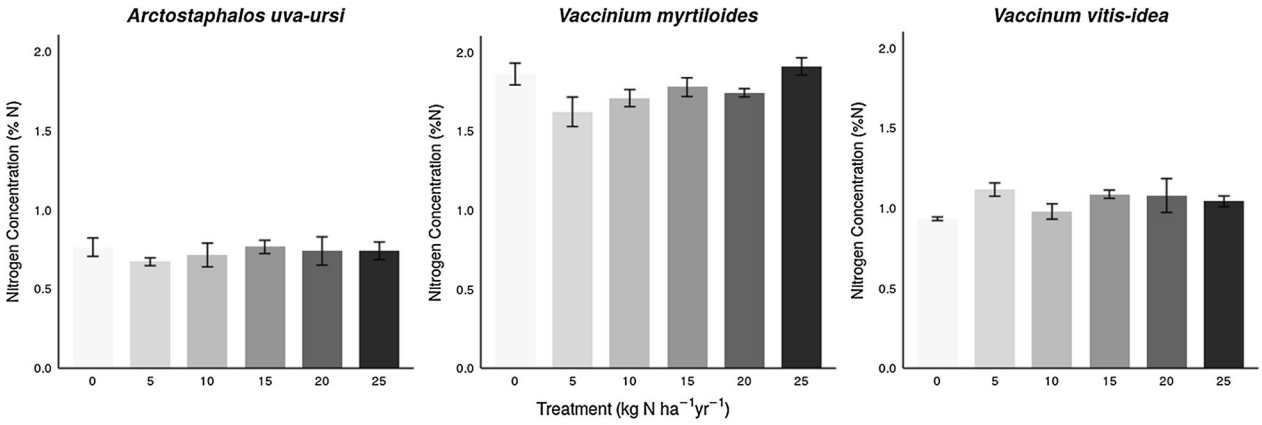

Fig. 4. N concentration (N%) of the three dominant dwarf shrubs in the area (*Arctostaphalos uva-ursi*, *Vaccinium myrtilloides*, and *Vaccinium vitis-idaea*) measured in 2015. Value shown for *Vaccinium vitis-idaea* at treatment 10 is an average of $n = 2$ due to accidental sample destruction.

Average foliar concentrations measured at 0 kg ha^{-1} y^{-1} in *Vaccinium vitis-idaea, Vaccinium myrtilloides,* and *Arctostaphylos uva-ursi* were about 1.0, 1.5, and 1.6%, respectively. This compares to average thalli concentrations measured at 0 kg ha^{-1} y^{-1} in *Cladonia mitis* of about 0.40%.

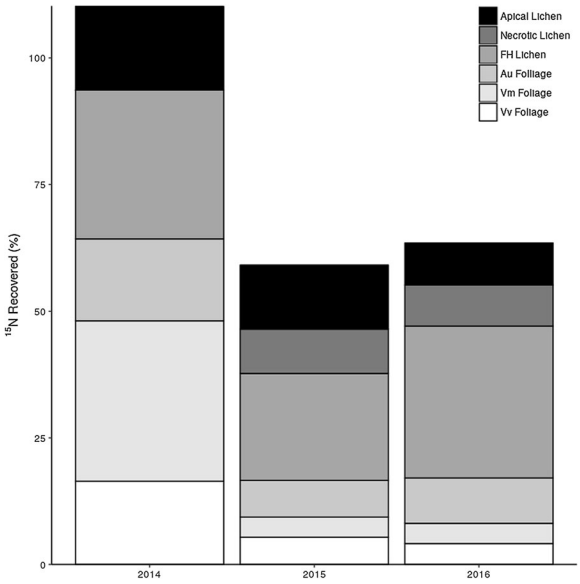

Fig. 5. Percent recovery of applied ^{15}N tracer in 2014, 2015, and 2016 in each measured biomass type.

^{15}N Enrichment and Total Recovery

Total recovery of ^{15}N tracer immediately following application was 110% of total applied with a followed by a decline and stabilization in the following two years (Figure 5). Initial ^{15}N recovery from apical lichen tissue immediately following application (2014) was 16.6% of total ^{15}N, which declined to 12.6% in 2015 and 8.3% in 2016. Recovery of ^{15}N in necrotic tissue in 2015 was 8.8% of total applied, which declined to 8.1% in 2016. Unfortunately, necrotic lichen tissue was omitted from sampling immediately following tracer application in 2014. Actual total recovery would likely have exceeded 110% had necrotic lichen been included. FH material represented one of the largest sinks for ^{15}N following isotope application. In 2014, 29.4% of applied ^{15}N was stored in FH tissue and by 2015 this proportion dropped to 21.1%. In 2016 however, the proportion grew to 30.0%. This increase occurred despite the FH material enrichment being relatively low (Figure 6). The high proportion of recovery in FH material is a function of mass rather than concentration. Apical and necrotic tissues were much more enriched with ^{15}N when compared with background tissues; however, their absolute mass is substantially less.

Dwarf shrub species also showed strong initial uptake and subsequent retention of ^{15}N, although there

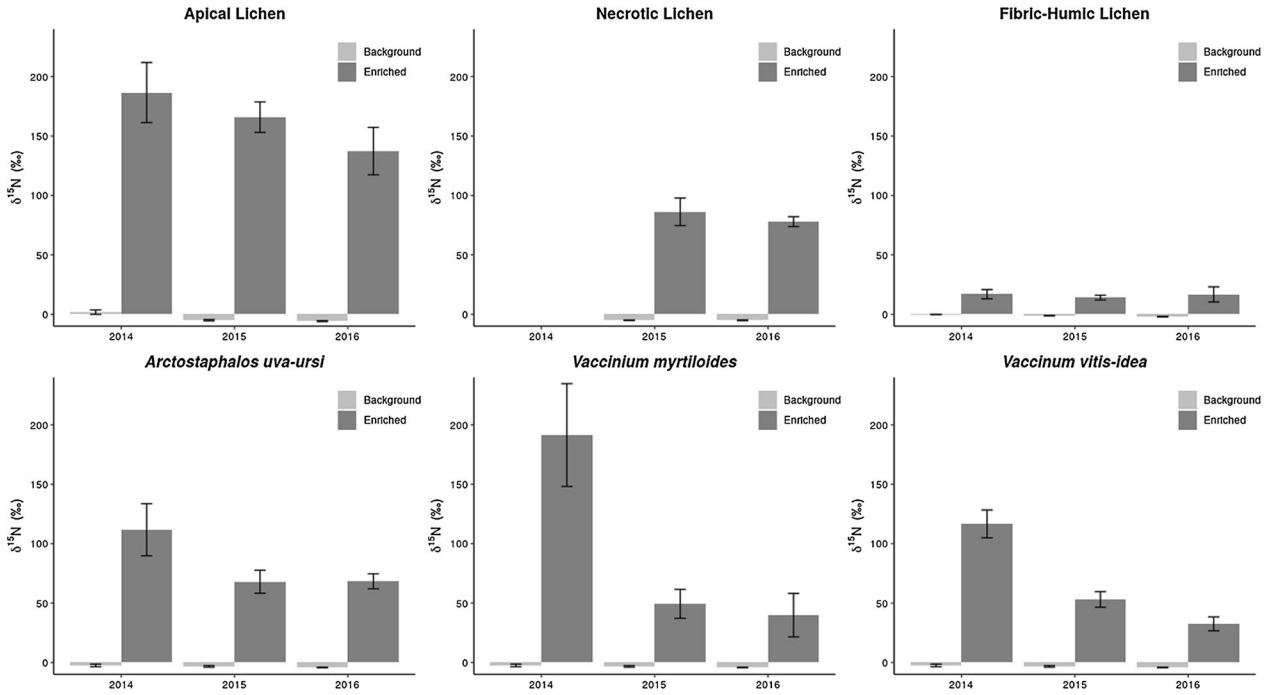

Fig. 6. Comparison of ^{15}N concentration of *Cladonia mitis* tissue (apical, necrotic, fibric–humic) and three ground vegetation species (*Arctostaphylos uva-ursi*, *Vaccinium myrtilloides*, *Vaccinium vitis-idaea*) (2014, 2015, 2016).

was considerable variation among species. *Vaccinium myrtilloides* foliage (Vm) had the greatest initial uptake with 31.7% of applied ^{15}N followed by a substantial decline to 4.0% in 2015 and the same amount in 2016. *Vaccinium vitis-idaea* foliage (Vv) initially took up 16.4% of applied ^{15}N which decreased to 5.4% in 2015 and 4.1% in 2016. *Arctostaphylos uva-ursi* (Au) interacted to applied ^{15}N similarly to *Vaccinium vitis-idaea,* with an initial uptake of 16.1% followed by a decrease to 7.2% in 2015 and 9.0% in 2016.

During the ^{15}N tracer experiment, the only biomass types that showed an increase in ^{15}N recovery from one year to another were *Arctostaphylos uva-ursi* and the FH horizon. The proportion of unrecovered ^{15}N in the FH horizon increased to 41.0% in 2015. Total recovery increased between 2015 and 2016, resulting in a decrease in the unrecovered proportion to 36.6%. Mineral soil samples were also analyzed from the Ae and B horizons, but the concentration of ^{15}N was below instrument detection limit. It is possible that some of the apparent loss of ^{15}N between initial application in 2014 and subsequent sampling in 2015–2016 is caused by leaching into the relatively massive mineral soil horizons. These coarse-textured soil horizons are sufficiently large to dilute tracer signatures beyond detection (Abdelbaki 2018).

Soil Microbial Communities

A PCR assay for the functional gene *amoA* performed on mineral soil (top 2 cm Ae horizon) failed to amplify product (Figure 7; top) at both 1/10 original DNA concentration and 1/100 original DNA concentration. The clear band produced from control sample DNA (from an Ontario forest soil) shows that the PCR was performed correctly and that product amplification was possible in a sample with known target DNA. This preliminary assay shows that microorganisms containing the *amoA* gene were not present in the mineral soil in detectable quantities. These results were confirmed by repeating this process with additional *amoA* primer sets producing the same result.

Bacterial or fungal abundances were not significantly affected by treatment (Figure 8). However, when expressed as fungal/bacterial ratios, there was a significant treatment effect ($p < 0.05$) although a very marginal one with fungal/bacterial ratios being generally lower at N treatments above 15 kg ha^{-1} y^{-1} (Figure 8). The seasonal effect was also less significant when expressed as ratios ($p < 0.05$), indicating that measured differences in bacterial and fungal communities between treatment sites may be largely attributable to site-specific variation in total microbial biomass.

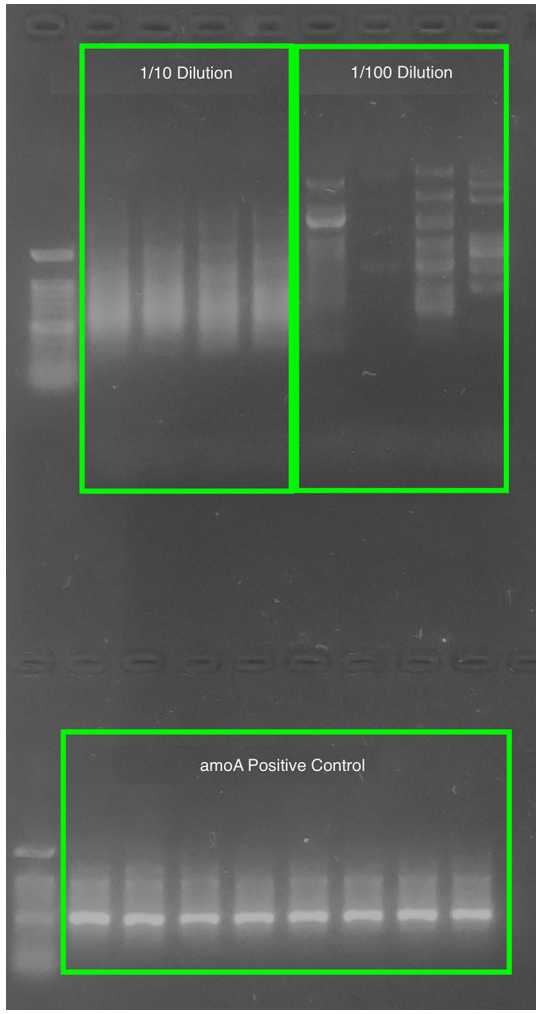

Fig. 7. Agarose gel showing results of PCR assay amoA functional gene in mineral soil (0–5 cm).

Discussion

Lichen Chemistry and Nutrient Balances

After 5 years of N additions, there was an increase in lichen N concentration that was most evident in the apical tissue but was also observed in necrotic tissue. Apical N concentrations were up to two times higher in the high N treatments (25 kg ha^{-1} y^{-1}) compared with the controls (0 kg ha^{-1} y^{-1}). It has been well established that lichen thalli N concentrations respond to atmospheric N deposition (Greenfield 1992; Hyvärinen and Crittenden 1998). Separation of lichen mats by depth showed that in addition to accumulating N in biologically active apical tissue, lichens also accumulate N in

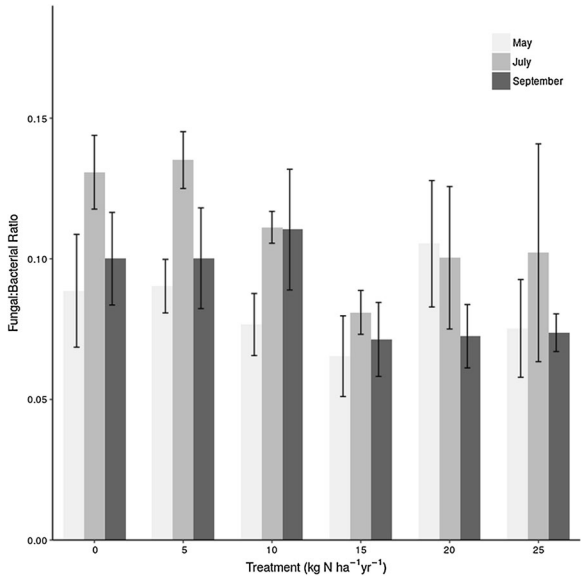

Fig. 8. Fungal/bacterial ratio of microbial communities in mineral soil between treatments in the 2015 growing season (May 2015, July 2015, September 2015).

their underlying necrotic tissue. The concentration of N was only marginally lower in necrotic than in apical tissue across all treatments. Wider disparities in apical and necrotic tissue N concentrations have been found in the terricolous lichen *Cladonia portentosa* in the UK, where N concentrations were 2–5 times greater in the upper thallus (apical) than the lower thallus (necrotic) (Hyvärinen and Crittenden 1998). The wider disparity between upper thallus and lower thallus N concentrations in *Cladonia portentosa* may be attributed to it being a much taller lichen than *Cladonia mitis*. A larger lichen thallus may allow for a more pronounced N concentration gradient to be formed across the length of the lichen structure.

There is strong evidence that terricolous lichens can translocate N and other nutrients through their thallus via passive transport (Nieboer and others 1978; Ellis and others 2005). This pattern of passive transport has been observed in the lichen *Cladonia alpestris* using ^{90}Sr and ^{137}Cs isotopes. When administered to the lower lichen thallus, the tracer was found to diffuse to the uppermost portion of the thallus (Tuominen 1967; Nieboer and others 1978). Nitrogen translocation in lichens has also been investigated using ^{15}N tracer studies by Kytöviita and Crittenden (2007) who found that N applied at the thallus base can be translocated upwards, but not the opposite. This movement is likely the result of intracellular diffusion, but the rates of tracer movement are consistent with cytoplasmic streaming rates which have been observed in other fungi (Bago and others 2002; Kytöviita and Crittenden 2007). Regardless of the mechanism of internal N translocation in lichen, it has been suggested that this process follows a source–sink relationship, in which the underlying lichen material acts as a source and new apical tissue acts as a sink. Hyvärinen and Crittenden (1998) suggest that atmospheric deposition and subsequent uptake of N by the apical lichen tissue may reduce the relative strength of the source–sink relationship, causing an increase in N accumulation in underlying lichen tissue (reduction in flux from necrotic to apical tissue). Another explanation for these patterns may simply be that necrotic lichen is intercepting N which passes through the apical layer directly. Enrichment of necrotic lichen may also occur via leaching of N from the apical thalli, or via the flushing of trapped particulates to lower strata of the lichen mat (Nieboer and others 1978). The FH material has a greater N concentration and is substantially larger than the apical and necrotic material, resulting in a N pool approximately 10 times larger than that of the apical and necrotic lichen. Due to the relatively large size of the FH N pool, and the high variability of fibric–humic mass from site to site, increases in N concentration in fibric–humic material did not measurably change the magnitude of the N pool in FH material in the timespan of this study.

Soil N Processes and Microbial Activity

After five years of N application, there was no significant response in net mineralization or net nitrification rates, although distinct seasonal patterns were observed. In temperate forest systems, the net mineralization rate has been found to increase with soil N concentration even beyond the point of N saturation (Perakis and Sinkhorn 2011). Results from the NITREX experiments in European boreal forests showed an intermediate response of mineralization rate and nitrification rate to N additions, in addition to a rapid increase in NO_3^- leaching (Tietema and others 1998a). Soil incubation experiments conducted as part of NITREX showed that in soils with variable N status, net mineralization rates were correlated with soil respiration (Tietema and others 1998a). The rapid release of NO_3^- despite only moderate increases in mineralization and nitrification in this study was attributed to the occurrence of mass flow events flushing added NO_3^- from the soil profile (Tietema and others 1998b). This suggests that the controls

on N saturation processes may be highly variable by region and ecosystem type. In particular, the N retention capacity of the ecosystem may influence the timespan over which N saturation occurs, and the type of saturation symptoms that manifest (Tietema and others 1998a). Mineralization rates may also be influenced by changes in soil moisture content. Beier and others (2008) found that N mineralization followed a parabolic trend as soil moisture increased, with peak N mineralization occurring at about 50% soil moisture. Soil moisture was not assessed at our sites, but the region is considered water-limited in general, receiving only 455 mm y^{-1} of precipitation.

It appeared that microbes possessing the *amoA* gene are not present in detectable quantities in the mineral soil at these study sites. The absence of nitrifying microbes in boreal forests has also been documented before (Ste-Marie and Paré 1999). An incubation study using soil from five different forest stands in northwestern Quebec showed that nitrification was extremely limited in soil from jack pine stands, when compared with paper birch, trembling aspen, white spruce and white cedar *(Thuja occidentalis)* even when controlling for soil properties (Ste-Marie and Paré 1999). Interestingly, when jack pine soil was amended with soil from another stand, nitrification was stimulated, suggesting that the microbial populations were not just dormant, but absent in jack pine forest soil (Ste-Marie and Paré 1999). In this study, the addition of NH_4^+ did not have a positive effect on nitrification rate, but increasing the pH elsewhere increased the nitrification rate (Ste-Marie and Paré 1999). Ste-Marie and Paré (1999) identified the soil pH threshold that allowed nitrification to proceed to be 5.3. This pH threshold is consistent with our pH measurements which were all below 5.3 in the FH and Ae horizons (Table 1). A soil reclamation study conducted in the AOSR found that reconstructed soils amended with peat had positive increases in N transformation rates (Masse and others 2016). In this study, the increases in N transformations were attributed to increases in organic N availability (Masse and others 2016). Soil pH in the reclamation study was consistently above the 5.3 threshold identified by Ste-Marie and Paré 1999, ranging between 5.9 and 7.2 (Masse and others 2016).

Denitrification was not directly measured in our study. Although forest soils are often aerobic, soil aggregates can produce anaerobic microsites which play host to denitrifying microbes (Keiluweit and others 2017). If significant denitrification was occurring, it may represent an important ''release valve'' for lichen-dominated systems experiencing the effects of N saturation. However, it is unlikely that denitrification represents a significant flux of N from the mineral soil since measured soil NO_3^- concentrations were negligible, and evidence of nitrifying microbes was not detected. Similarly, soil N_2O emissions measured from jack pine forest in northern Saskatchewan have shown that under background conditions, emissions are quite negligible (0.005–0.008 g N_2O–N m^{-2} y^{-1}) (Matson and others 2009).

As systems become N saturated, soils microbial communities have been found to shift from fungal dominance to bacterial dominance (Strickland and Rousk 2010). In turn, gross mineralization has been found to decrease as fungi/bacterial ratio decreases as well, supporting the current understanding that bacterial communities are disproportionality responsible for N transformation processes (Högberg and others 2007). Increasing N addition slightly reduced the ratio of fungi/bacteria as determined via qPCR. Soil fungi/bacterial ratios measured via phospholipid fatty acid (PLFA) analysis have been found to be negatively correlated with distance in the AOSR across a N deposition gradient originating at the industrial center (Masse and others 2015). However, our study did not measure a corresponding change in net mineralization rate. Therefore, it is likely that mineralization rate was limited by another factor beyond fungi/bacterial ratio. Högberg and others (2007) found a positive correlation between soil pH and gross mineralization, and a negative relationship between soil C:N and gross mineralization. The pH values measured in the mineral soil at the study sites were low, ranging from 4.76 to 5.05 (Table 1). Based on their relationship, the soil C:N is likely the strongest limiting factor on mineralization rate at the study location.

Integration of Added Nitrogen into the Local N Cycle

^{15}N enrichment of apical lichen tissue, necrotic tissue, and FH material was largely consistent with expectations from the N concentrations of the separated lichen mats. The initial total recovery of ^{15}N was very high (110.24%), which is consistent with many ^{15}N tracer studies which routinely exceed 100% due to high variability (Templer and others 2012). The actual total recovery is likely much larger still, considering that the necrotic lichen pool was initially omitted from sampling in 2014. Apical lichen tissue had the second highest concentration of ^{15}N immediately following enrichment and had high retention of the initial

enrichment year-to-year. The FH material had the lowest initial ^{15}N concentration in 2014 and remained essentially unchanged during subsequent measurements in 2015 and 2016. However, when ^{15}N in the FH material is expressed in terms of total recovery, FH material is clearly the largest N pool, which is consistent with other tracer studies (Templer and others 2012).

^{15}N tracer results showed that the initial uptake of N to dwarf shrubs is greater than anticipated based upon N concentration measurements. High initial ^{15}N concentrations may have been influenced by direct application in our experiment and therefore may simply represent surface residue rather than physiological uptake. It was assumed that dwarf shrub uptake of N was low because the preliminary N concentrations measured in dwarf shrubs in 2015 showed that that after five years of N addition, there were no statistically significant differences in N concentrations with treatment. The dwarf shrubs *Vaccinium vitis-idaea* and *Arctostaphalos uva-ursi* both accumulated a moderate amount of ^{15}N immediately after application followed by a large decrease from 2014 to 2015. In the second year after application, the ^{15}N concentration was largely stable. This contrasts with the third dwarf shrub *Vaccinium myrtilloides* that accumulated the most ^{15}N immediately after application, but then also experienced the most dramatic loss of ^{15}N from year 1 to year 3. High initial ^{15}N tracer uptake has also been measured in the closely related species *Vaccinium myrtillus* (Nordin and others 1998). Some of the discrepancy between the dwarf shrub ^{15}N uptake and retention may be attributed to their differences in physiology. *Vaccinium vitis-idaea* and *Arctostaphylos uva-ursi* are both evergreen shrubs with waxy-textured leaves that are retained for 1–3 years, whereas *Vaccinium myrtilloides* loses its foliage annually. Others have shown that dwarf shrub response to N addition is largely controlled by foliage type (wintergreen, evergreen, deciduous) (Baddeley and others 1994; Parsons and others 1994). Studies have also shown that dwarf shrub response to N additions can be highly sensitive to exposure to either wet or dry deposition sources (Phoenix and others 2012). Species-specific re-translocation or uptake of ^{15}N tracer from the FH material or soil pools may also attribute to the differences between dwarf shrub responses in 2015–2016.

^{15}N enrichment in the FH was observable immediately after application in 2014, but measurements of FH material in 2015 after 5 years of N additions did not show a broad treatment effect on N concentration. This is further evidence that the large size of the FH material N pool caused it to be resistant to changes in measurable concentration from incoming N additions. Another feature of the FH shown by the ^{15}N tracer experiment is that the pool concentration was almost unchanged year-to-year, but the total recovery of ^{15}N between 2015 and 2016 increased. This could be the result of the slow integration of lichen and dwarf shrub biomass into the FH material through decomposition. Over time the N in the FH horizon will likely become incorporated into the mineral soil, but mineral soil (Ae and B horizon) ^{15}N enrichment in this study could not be detected as the concentration was below the detection limit of the instrument. Others have suggested that the mineral soil may account for large amounts of unrecovered tracer in boreal experiments (Nordin and others 1998).

Implications for N Saturation and Critical Loads

After five years of experimental N deposition in a boreal forest system of northern Alberta, the traditional hypothesized patters of N saturation put forward by Aber and others (1989) have largely not been observed. The strongest response to increased N deposition has been a steady accumulation of N in the apical tissue and necrotic tissue of the terricolous lichen *Cladonia mitis* and *Cladonia stellaris.* Slight effects of treatment on microbial communities may represent an early sign of response, although more robust study is required. When the results of the three lines of evidence are synthesized, numerous potential N mobility pathways in the forest floor are evident (Figure 9). These observations are consistent with the N-saturation model put forward by Lovett and Goodale (2011). In the context of the Lovett and Goodale model, N deposition is initially partitioned into the soil lichen/vegetation pool and the soil FH pool. Based on measurements of mineralization rate, nitrification rate, and soil microbial guilds, N losses due to leaching are negligible. Denitrification, although not directly measured, is also unlikely to be occurring in significant quantities.

It is proposed that at the sites examined in this study, *Cladonia mitis* apical and, to a lesser extent, necrotic tissue is progressing toward a state of capacity N saturation, which will be characterized by physiological decline of the lichen thallus and lichen death, whereas the uptake pathways of *Vaccinium myrtilloides, Vaccinium vitis-idaea,* and *Arctostaphylos uva-ursi* are experiencing kinetic N saturation. If the dominant uptake pathway for dwarf shrubs is through foliar deposition, kinetic

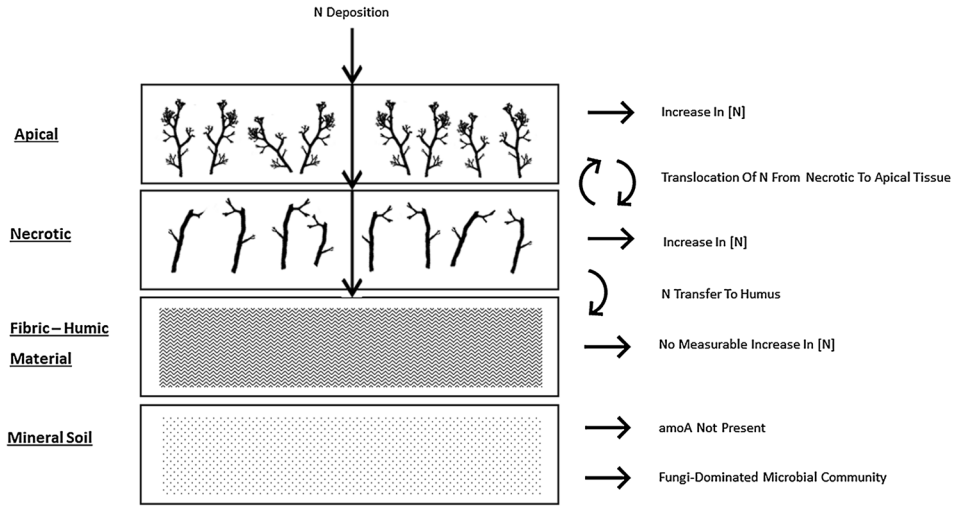

Fig. 9. Conceptual diagram of the response to N addition in the forest floor.

saturation of this pathway would explain the discrepancy between high enrichment of ^{15}N in *Arctostaphylos uva-ursi* foliage in the tracer experiment, despite the absence of a treatment response in total N concentration. *Arctostaphylos uva-ursi* would be unable to take advantage of increased N deposition and foliar N would not continue to increase year-over-year. Under this framework, the N accumulation rate for dwarf shrubs is limited by the foliar uptake pathway, with physiological variations between evergreen and deciduous shrubs (Baddeley and others 1994; Parsons and others 1994). Lichens, by contrast, have an extremely high potential N accumulation rate and continue to respond to additional N. This assertion is consistent with findings which show that cumulative N load is more detrimental to terricolous lichen cover than N concentration in the long term (Britton and Fisher 2010). The presence of other potential contaminants (dust, metals: Watmough and others 2018) in the region may also contribute to declines in lichen health and so synergistic effects between N and other contaminants should not be ruled out.

Conclusion

This work has shown that the FH material which forms under terricolous lichen mats acts as a significant sink of atmospheric N deposition. The FH material moderates the release of N to mineral soil. Therefore, the continued growth of these mats is imperative for mitigating the effects of N saturation. The greatest risk to this system under N saturation is the loss of terricolous lichen cover as it reaches and exceeds its N-toxicity threshold. Without continued lichen growth and decomposition, the forest floor will lose the capacity to replenish its large humus layer. Simultaneously, the humus layer may begin to receive a greater flux of N as the density of lichen, and therefore, N retention capacity of apical and necrotic tissue declines. It can be expected that once the C/N ratio of the FH material decreases to a sufficient level; microbial populations will respond and accelerate rates of N conversion. N critical loads for the AOSR should be set to sufficiently protect terricolous lichens, as their growth and structure have a disproportionate effect on the regulation of N in boreal forests.

Acknowledgments

This work was funded by CEMA (Cumulative Environmental Management Association). The authors would like to thank our laboratory and field staff at Trent University: Sylvie Danse, Katie Mitchell, Eric Grimm, Liam Murray, Liana Orlovskaya, and Jaqueline London. We would also like to thank our close collaborators Shanti Berryman and Justin Straker of Integral Ecology Group.

References

Abdelbaki AM. 2018. Evaluation of pedotransfer functions for predicting soil bulk density for U.S. soils. Ain Shams Eng J 9(4):1611–19. https://doi.org/10.1016/j.asej.2016.12.002.

Aber JD, Nadelhoffer KJ, Steudler P, Melillo JM. 1989. Nitrogen saturation in northern forest ecosystem. Bioscience 39:378–86.

Akselsson C, Belyazid S, Hellsten S, Klarqvist M, Pihl-Karlsson G, Karlsson PE, Lundin L. 2010. Assessing the risk of N leaching from forest soils across a steep N deposition gradient in Sweden. Environ Pollut 158:3588–95.

Allison SD, Czimczik CI, Treseder KK. 2008. Microbial activity and soil respiration under nitrogen addition in Alaskan boreal forest. Glob Change Biol 14:1156–68.

Baddeley JA, Woodin SJ, Alexander IJ, Ecology F, Dec N. 1994. Effects of increased nitrogen and phosphorus availability on the photosynthesis and nutrient relations of three arctic dwarf shrubs from Svalbard. Funct Ecol 8:676–85.

Bago B, Zipfel W, Williams RM, Jun J, Arreola R, Lammers PJ, Pfeffer PE, Shachar-Hill Y. 2002. Translocation and utilization of fungal storage lipid in the arbuscular mycorrhizal symbiosis. Plant Physiol 128:108–24.

Baptista JDC, Lunn M, Davenport RJ, Swan DL, Read LF, Brown MR, Morais C, Curtis TP. 2014. Agreement between amoA gene-specific quantitative PCR and fluorescence in situ hybridization in the measurement of ammonia-oxidizing bacteria in activated sludge. Appl Environ Microbiol 80:5901–10.

Beier C, Emmett BA, Peñuelas J, Schmidt IK, Tietema A, Estiarte M, Gundersen P, Llorens L, Riis-Nielsen T, Sowerby A, Gorissen A. 2008. Carbon and nitrogen cycles in European ecosystems respond differently to global warming. Sci Total Environ 407:692–7.

Bobbink R, Hicks K, Galloway J, Spranger T, Alkemade R, Ashmore M, Bustamante M, Cinderby S, Davidson E, Dentener F, Emmett B, Erisman JW, Fenn M, Gilliam F, Nordin A, Pardo L, De Vries W. 2010. Global assessment of nitrogen deposition effects on terrestrial plant diversity: a synthesis. Ecol Appl 20:30–59.

Britton AJ, Fisher JM. 2010. Terricolous alpine lichens are sensitive to both load and concentration of applied nitrogen and have potential as bioindicators of nitrogen deposition. Environ Pollut 158:1296–302.

Bytnerowicz A, Fraczek W, Schilling S, Alexander D. 2010. Spatial and temporal distribution of ambient nitric acid and ammonia in the Athabasca Oil Sands Region, Alberta. J Limnol 69:11–21.

Canada E. 2011. Station results—historical data. http://climate.weather.gc.ca/climateData/dailydata_e.html?StationID=27216. Accessed June 2015.

Cornelissen JHC, Callaghan TV, Alatalo JM, Michelsen A, Graglia E, Hartley AE, Hik DS, Hobbie SE, Press MC, Robinson CH, Henry GHR, Shaver GR, Phoenix GK, Jones DG, Jonasson S, Chapin FS, Molau U, Neill C, Lee JA, Melillo JM, Sveinbjörnsson B, Aerts R. 2001. Global change and arctic ecosystems: is lichen decline a function of increases in vascular plant biomass? J Ecol 89:984–94.

Crittenden PD. 1991. Ecological significance of necromass production in mat-forming lichens. Lichenol 23:323–31.

Demoling F, Ola Nilsson L, Bååth E. 2008. Bacterial and fungal response to nitrogen fertilization in three coniferous forest soils. Soil Biol Biochem 40:370–9.

Dick WA, Tabatabai MA. 1979. Ion chromatographic determination of sulfate and nitrate in soils 1. Soil Sci Soc Am J 43:899–904.

Driscoll CT, Whitall D, Aber J, Elizabeth Boyer MC, Cronan C, Goodale CL, Peter Groffman CH, Lambert K, Gregory Lawrence ASO. 2003. Nitrogen pollution in the northeastern United States: sources, effects, and management options. Bioscience 53:357–74.

Ellis CJ, Crittenden PD, Scrimgeour CM, Ashcroft C. 2003. The natural abundance of 15N in mat-forming lichens. Oecologia 136:115–23.

Ellis CJ, Crittenden PD, Scrimgeour CM, Ashcroft CJ. 2005. Translocation of 15N indicates nitrogen recycling in the mat-forming lichen *Cladonia portentosa*. New Phytol 168:423–34.

Emmett BA, Boxman D, Bredemeier M, Gundersen P, Kjønaas OJ, Moldan F, Schleppi P, Tietema A, Wright RF. 1998. Predicting the effects of atmospheric nitrogen deposition in conifer stands: evidence from the NITREX ecosystem-scale experiments. Ecosystems 1:352–60.

Fenn ME, Bytnerowicz A, Schilling SL, Ross CS. 2015. Atmospheric deposition of nitrogen, sulfur and base cations in jack pine stands in the Athabasca Oil Sands Region, Alberta, Canada. Environ Pollut 196:497–510.

Fenn ME, Nagel HD, Koseva I, Aherne J, Jovan SE, Geiser LH, Schlutow A, Scheuschner T, Bytnerowicz A, Gimeno BS, Yuan F, Watmough SA, Allen EB, Johnson RF, Meixnert T. 2014. A comparison of empirical and modelled nitrogen critical loads for mediterranean forests and shrublands in California. Nitrogen Depos Crit Loads Biodivers Proc Int Nitrogen Initiat Work Link Expert Conv Long-Range Transbound Air Pollut Conv Biol Divers. pp 357–68.

Fenn MME, Baron JSJ, Allen EBE, Rueth HMH, Nydick KRK, Geiser L, Bowman WWD, Sickman JJO, Meixner T, Johnson DDW, Neitlich P. 2003. Ecological effects of nitrogen deposition in the western United States. Bioscience 53:404.

Fierer N, Jackson J. 2005. Assessment of soil microbial community structure by use of taxon-specific quantitative PCR assays. Appl Environ Microbiol 71:4117.

Galloway JN, Dentener FJ, Capone DG, Boyer EW, Howarth RW, Seitzinger SP, Asner GP, Cleveland CC, Green PA, Holland EA, Karl DM, Michaels AF, Porter JH, Townsend AR, Vörösmarty CJ. 2004. Nitrogen cycles: past, present, and future. Biogeochemistry 70:153–226.

Glass NL, Donaldson GC. 1995. Development of primer sets designed for use with the PCR to amplify conserved genes from filamentous ascomycetes. Appl Environ Microbiol 61:1323–30.

Greenfield LG. 1992. Short note retention of precipitation nitrogen by Antarctic mosses, lichens and fellfield soils. Antarct Sci 4:205–6.

Hart SC, Nason GE, Myrold DD, Perry DA. 1994. Dynamics of gross nitrogen transformations in an old-growth forest: the carbon connection. Ecology 75:880–91.

Högberg MN, Bååth E, Nordgren A, Arnebrant K, Högberg P. 2003. Contrasting effects of nitrogen availability on plant carbon supply to mycorrhizal fungi and saprotrophs—a hypothesis based on field observations in boreal forest. New Phytol 160:225–38.

Högberg MN, Chen Y, Högberg P. 2007. Gross nitrogen mineralisation and fungi-to-bacteria ratios are negatively correlated in boreal forests. Biol Fertil Soils 44:363–6.

Hyvärinen M, Crittenden PD. 1998. Relationships between atmospheric nitrogen inputs and the vertical nitrogen and phosphorus concentration gradients in the lichen *Cladonia portentosa*. New Phytol 140:519–30.

Keiluweit M, Wanzek T, Kleber M, Nico P, Fendorf S. 2017. Anaerobic microsites have an unaccounted role in soil carbon stabilization. Nat Commun 8:1–8.

Kytöviita MM, Crittenden PD. 2007. Growth and nitrogen relations in the mat-forming lichens *Stereocaulon paschale* and *Cladonia stellaris*. Ann Bot 100:1537–45.

Levy-Booth DJ, Prescott CE, Grayston SJ. 2014. Microbial functional genes involved in nitrogen fixation, nitrification

and denitrification in forest ecosystems. Soil Biol Biochem 75:11–25.

Lovett GM, Goodale CL. 2011. A new conceptual model of nitrogen saturation based on experimental nitrogen addition to an oak forest. Ecosystems 14:615–31.

Masse J, Prescott CE, Müller C, Grayston SJ. 2016. Gross nitrogen transformation rates differ in reconstructed oil-sand soils from natural boreal-forest soils as revealed using a15N tracing method. Geoderma 282:37–48.

Matson A, Pennock D, Bedard-Haughn A. 2009. Methane and nitrous oxide emissions from mature forest stands in the boreal forest, Saskatchewan, Canada. For Ecol Manag 258:1073–83.

Mitchell RJ, Truscot AM, Leith ID, Cape JN, Van Dijk N, Tang YS, Fowler D, Sutton MA. 2005. A study of the epiphytic communities of Atlantic oak woods along an atmospheric nitrogen deposition gradient. J Ecol 93:482–92.

Munzi S, Sheppard LJ, Leith ID, Cruz C, Branquinho C, Bini L, Gagliardi A, Cai G, Parrotta L. 2017. The cost of surviving nitrogen excess: energy and protein demand in the lichen *Cladonia portentosa* as revealed by proteomic analysis. Planta 245:819–33.

Nadkarni M, Martin FE, Jacques NA, Hunter N. 2002. Determination of bacterial load by real-time PCR using a broad range (universal) probe and primer set. Microbiology 148:257–66.

Neuwirth E. 2014. RColorBrewer: ColorBrewer palettes. R Package version 11–2:https://cran.R-project.org/package=RColorBrewer. Accessed Aug 2017.

Nieboer E, Richardson DHS, Tomassini FD. 1978. Mineral uptake and release by lichens: an overview. Bryologist 81:226–46.

Nihlgard B. 1985. The ammonium hypothesis: an additional explanation to the forest dieback in Europe. Ambio 14:2–8.

Nordin A, Näsholm T, Ericson L. 1998. Effects of simulated N deposition on understorey vegetation of a boreal coniferous forest. Funct Ecol 12:691–9.

Pardo LH, Templer PH, Goodale CL, Duke S, Groffman PM, Adams MB, Boeckx P, Boggs J, Campbell J, Colman B, Compton J, Emmett B, Gundersen P, Kjønaas J, Lovett G, Mack M, Magill A, Mbila M, Mitchell MJ, McGee G, McNulty S, Nadelhoffer K, Ollinger S, Ross D, Rueth H, Rustad L, Schaberg P, Schiff S, Schleppi P, Spoelstra J, Wessel W. 2006. Regional assessment of N saturation using foliar and root δ15N. Biogeochemistry 80:143–71.

Parsons AN, Welker JM, Wookey PA, Press MC, Callaghan TV, Lee JA, Press JMC, Lee AA. 1994. Growth responses of four sub-Arctic dwarf shrubs to simulated environmental change. J Ecol 82:307–18.

Perakis SS, Sinkhorn ER. 2011. Biogeochemistry of a temperate forest nitrogen gradient. Ecology 92:1481–91.

Phoenix GK, Emmett BA, Britton AJ, Caporn SJM, Dise NB, Helliwell R, Jones L, Leake JR, Leith ID, Sheppard LJ, Sowerby A, Pilkington MG, Rowe EC, Ashmore MR, Power SA. 2012. Impacts of atmospheric nitrogen deposition: responses of multiple plant and soil parameters across contrasting ecosystems in long-term field experiments. Glob Change Biol 18:1197–215.

R Core Team. 2017. R: a language and environment for statistical computing. R Found Stat Comput. Vienna, Austria. https://www.R-project.org. Accessed Nov 2017.

Robinson D. 2001. δ 15N as an integrator of the nitrogen. Trends Ecol Evol 16:153–62.

Robinson D. 2017. broom: convert statistical analysis objects into tidy data frames. R package version 0.4.3.

Rotthauwe JH, Witzel KP, Liesack W. 1997. The ammonia monooxygenase structural gene amoA as a functional marker: molecular fine-scale analysis of natural ammonia-oxidizing populations. Appl Environ Microbiol 63:4704–12.

Soil Classification Working Group. 1998. The Canadian System of Soil Classification. Can Syst Soil Classif, 3rd ed, Agric Agri-Food Canada Publ 1646:187.

Ste-Marie C, Paré D. 1999. Soil, pH and N availability effects on net nitrification in the forest floors of a range of boreal forest stands. Soil Biol Biochem 31:1579–89.

Stephen JR, Chang YJ, Macnaughton SJ, Kowalchuk GA, Leung KT, Flemming CA, White DC. 1999. Effect of toxic metals on indigenous soil β-subgroup proteobacterium ammonia oxidizer community structure and protection against toxicity by inoculated metal-resistant bacteria. Appl Environ Microbiol 65:95–101.

Strickland MS, Rousk J. 2010. Considering fungal: bacterial dominance in soils - Methods, controls, and ecosystem implications. Soil Biol Biochem 42:1385–95.

Templer PH, Mack MC, Chapin FS, Christenson LM, Compton JE, Crook HD, Currie WS, Curtis CJ, Dail DB, D'Antonio CM, Emmett BA, Epstein HE, Goodale CL, Gundersen P, Hobbie SE, Holland K, Hooper DU, Hungate BA, Lamontagne S, Nadelhoffer KJ, Osenberg CW, Perakis SS, Schleppi P, Schimel J, Schmidt IK, Sommerkorn M, Spoelstra J, Tietema A, Wessel WW, Zak DR. 2012. Sinks for nitrogen inputs in terrestrial ecosystems: a meta-analysis of 15N tracer field studies. Ecology 93:1816–29.

Tietema A, Boxman AW, Bredemeier M, Emmett BA, Moldan F, Gundersen P, Schleppi P, Wright RF. 1998a. Nitrogen saturation experiments (NITREX) in coniferous forest ecosystems in Europe: a summary of results. Environ Pollut 102:433–7.

Tietema A, Emmett BA, Gundersen P, Janne Kjønaas O, Koopmans CJ. 1998b. The fate of 15N-labelled nitrogen deposition in coniferous forest ecosystems. For Ecol Manag 101:19–27.

Tuominen Y. 1967. Studies on the strontium uptake of the *Cladonia alpestris* thallus. In: Annales Botanici Fennici. JSTOR. pp 1–28.

Wallenstein MD, McNulty S, Fernandez IJ, Boggs J, Schlesinger WH. 2006. Nitrogen fertilization decreases forest soil fungal and bacterial biomass in three long-term experiments. For Ecol Manage 222:459–68.

Watmough SA, Bird A, Mcdonough A, Grimm E. 2018. Forest fertilization associated with oil sands emissions. Ecosystems 1–14. https://doi.org/10.1007/s10021-018-0249-x.

Watmough SA, Whitfield CJ, Fenn ME. 2014. The importance of atmospheric base cation deposition for preventing soil acidification in the Athabasca Oil Sands Region of Canada. Sci Total Environ 493:1–11.

Wickham H. 2016. ggplot2. Create elegant data visualizations using the grammar of graphics. R package version 2.1.0. https://cran.r-project.org/web/packages/ggplot2/index.html. Accessed June 2016.

Wright RF, van Breemen N. 1995. The (NITREX) project: an introduction. For Ecol Manage 71(1-2):1–5. https://doi.org/10.1016/0378-1127(94)06080-3.